IOPscience iopscience.iop.org

Home Search Collections Journals About Contact us My IOPscience

The optical properties of the Nd^{3+} ion in $NdGaO_3$ and $LaGaO_3$:Nd: temperature and concentration dependence

This article has been downloaded from IOPscience. Please scroll down to see the full text article.

1995 J. Phys.: Condens. Matter 7 9657

(http://iopscience.iop.org/0953-8984/7/49/027)

View the table of contents for this issue, or go to the journal homepage for more

Download details:
IP Address: 171.66.16.151
The article was downloaded on 12/05/2010 at 22:42

Please note that terms and conditions apply.

J. Phys.: Condens. Matter 7 (1995) 9657–9673. Printed in the UK

The optical properties of the Nd^{3+} ion in $NdGaO_3$ and $LaGaO_3$:Nd: temperature and concentration dependence

V M Orera†, L E Trinkler‡, R I Merino† and A Larrea†

† Instituto de Ciencia de Materiales de Aragon (CSIC-UZ), Facultad de Ciencias, Universidad de Zaragoza, Zaragoza, Spain

‡ Institute of Solid State Physics, University of Latvia, Riga, Latvia

Received 24 May 1995, in final form 4 August 1995

Abstract. The energies of most of the f–f crystal-field levels of $NdGaO_3$ and neodymium-doped $LaGaO_3$ crystals are given. The oscillator strengths of the $J \rightarrow J'$ Nd^{3+} absorption bands and of some zero-phonon transitions between individual Stark crystalline states have been determined at temperatures between 9 and 300 K for both compounds. Within the frame of the Judd–Ofelt theory we have calculated the Nd^{3+} intensity parameters from the 300 K spectra. A comparison between the stoichiometric and the diluted material reveals a very large concentration enhancement of vibronic bands and an unusual and strong temperature dependence of some zero-phonon oscillator strengths in $NdGaO_3$. These phenomena point towards the existence of an enhanced electron–phonon interaction presumably related to the excited configuration, superexchange interaction between adjacent Nd^{3+} ions in the stoichiometric crystal. In $LaGaO_3$:Nd crystals we detected $^4F_{3/2}$ emission with a quantum efficiency close to unity and a temperature-independent lifetime of $\approx$250 μs. This emission is completely quenched in $NdGaO_3$.

1. Introduction

Oxide perovskites are simple systems with very interesting magnetic and electronic properties. In particular $NdGaO_3$ (NGO) is a magnetic insulator showing antiferromagnetic ordering at $T_c = 0.97$ K. The main contribution to the Nd–Nd interaction is due to magnetic superexchange which is much larger than the magnetic dipole–dipole interaction [1]. Furthermore, NGO and $LaGaO_3$ (LGO) crystals have proved to be suitable substrates for high-T_c superconducting films used in microwave devices because of their moderate dielectric constant and very low losses in the GHz frequency range [2, 3], together with the small lattice mismatch between these perovskites and the $YBa_2Cu_3O_x$ superconductor. These characteristics have stimulated recent work on the study of the physical properties of these compounds focusing mainly on the determination of their crystal structure [4, 5], infrared optical properties [6, 7], thermal expansion coefficients [8] and dielectric response [9]. Information on the electronic structure of these compounds is still very scarce. Recently Podlesnyak *et al* [4] studied the crystalline-electric-field (Stark levels) effect on the NGO ground state by inelastic neutron scattering. Up to now no such information is available for the excited states.

In addition there is much interest in the electronic properties of stoichiometric compounds, especially the effects resulting from the interactions between light absorbers. In fact when the concentration of optically active ions is high enough the electronic states may no longer be treated as single-ion states. Electronic interactions between ions may

0953-8984/95/499657+17$19.50 © 1995 IOP Publishing Ltd

produce bandlike states and excitonic transitions as well as energy-transfer effects (see for example reviews in [10–12] and references therein). The range of phenomena is very variable depending on both ion and host and general rules cannot be easily predicted from existing theories.

In general, exciton states, Davidov splittings and magnon sidebands in magnetic ordered crystals have been observed in fully concentrated, transition-metal-ion compounds. For rare-earth metal ions the main effect of the ion–ion interaction is to enhance energy-transfer processes which leads to strong luminescence concentration quenching effects (CQ) as well as to an increase in the probability of some vibronic transitions (see [13] and references therein). The situation concerning rare-earth ions is far from being clear. For example Eu^{3+} is a good luminscent ion in most of the studied materials, whereas Pr^{3+} generally shows strong CQ effects. Nd^{3+} compounds constitute an intermediate case in which luminescent properties depend critically on the environment of the metal ion [14].

In the present work we report the results obtained from optical absorption and emission measurements of these gallates. The crystals are of an optical quality in the visible and near-infrared spectral regions, which is good enough to allow us to use optical spectroscopy techniques to obtain information on the electronic structure of the excited states.

The compounds are orthorhombic perovskites, isostructural with $GdFeO_3$, and they belong to the space group D_{2h}^{16} with four formulae per unit cell for the measurement temperature range [15]. The lattice parameters a, b and c are 5.426, 5.502 and 7.706 Å, respectively, for NGO and 5.496, 5.524 and 7.787 Å, respectively, for LGO. The rare-earth ions occupy the 4c sites in the centre of strongly distorted oxygen dodecahedra (point group C_s). For a representation of the crystal structure see, for example, figure 1 in [4]. The Nd–O distances range from 2.3 to 3.4 Å and those for Nd–Nd between 3.8 and 3.95 Å. For LGO the Nd^{3+} impurity substitute for the rare-earth ion.

The $^{2S+1}L_J$ multiplets of the $4f^3$ configuration of Nd^{3+} are split by the low-symmetry crystal field into Kramers doublets. For NGO low-temperature optical absorption spectroscopy allows us to identify the energy position of most of these doublets over the 10 000 to 40 000 cm^{-1} range. We have also measured the transition oscillator strengths as a function of temperature and obtained the intensity parameters of this compound. A comparison with neodymium-doped LGO has revealed some interesting differences. In fact we have observed, in addition to a strong-luminescence CQ effect, an unusual temperature dependence of the zero-phonon transition probabilities and a concentration enhancement in the vibronic absorption spectrum of the stoichiometric compound. Our results point towards the existence of a large electron–phonon interaction in the concentrated system and we discuss its possible origin.

2. Experimental details and sample characterization

Optical absorption measurements were carried out with a Hitachi U-3400 spectrophotometer. Polarized optical absorption spectra in the 350–900 nm region were obtained using unsupported dichroic polarizers.

Photoluminescence spectra were recorded by exciting the sample with light from a 1000 W tungsten lamp passed through a 0.5 m double monochromator. Fluorescence was detected through a 0.5 m monochromator with a Si diode detector. Lifetime measurements were performed by modulating the exciting light with a mechanical chopper and using a Tektronic 2430 digital oscilloscope. Variable temperatures below 300 K were achieved using a closed-cycle cryorefrigerator with an accuracy of ±1 K.

The $NdGaO_3$ and Nd-doped $LaGaO_3$ crystals used in this study were grown by the flame fusion method. The NGO sample was a large, dark single crystal of excellent optical and mechanical quality. After orientation using the back-reflection Laue method, thin slabs parallel to the (110) planes of ≈ 100 mm$^2 \times 0.3$ mm were cut and polished. Light propagates in a direction perpendicular to the c-axis. For this configuration both σ- and π-polarizations can be measured. Unpolarized spectra correspond to the σ, π-configuration. The LGO boule was not a single crystal; it appeared as a clear, grey-coloured polycrystalline material with some small dark crystallites embedded in it.

Electron probe microanalysis (EPMA) of the LGO sample was done. The x-ray energy dispersive spectra were acquired with a Jeol 6400 scanning electron microscope (SEM) using a Link Analytical eXL system equipped with a Si(Li) solid-state detector (resolution at 5.9 keV: 137 eV). To perform the elemental analysis the sample was prepared by conventional techniques and irradiated by the SEM with a 20 keV electron microprobe; the x-ray spectrum was recorded during 600 s of live acquisition time. To obtain the chemical composition of the sample, profiles of the L peaks from the La and Nd atoms were prepared from spectra of pure metallic samples and the Ga K peak profile from an NGO sample. To quantify the spectrum, the peak profiles of the references were fitted to the sample spectrum and the apparent concentrations corrected by the ZAF iterative method.

We obtained the following results. The grey phase corresponded to the $La_2GaO_{4.5}$ compound whereas the dark crystallites had the desired LGO formula. The Nd impurity distributed itself quite inhomogeneously throughout the sample. We extracted from the boule some small, unoriented (≈ 1 mm^3) pieces of LGO that we used in the studies.

The Nd content of the crystallites was determined by recording 20 energy-dispersive spectra over different sample surface points. In particular the optical absorption and emission measurements were carried out for a sample with a Nd^{3+} concentration $(2.1 \pm 0.25) \times 10^{20}$ ions cm^{-3}.

A refractive index of 2.13 was estimated by the apparent thickness method using an optical microscope and white light for NGO. We assumed the same value for LGO.

3. Experimental results and interpretation

In the presence of a crystal field of C_s symmetry each $|J\rangle$ level of the $4f^3$ Nd^{3+} configuration splits into $(2J + 1)/2$ Kramers doublets. For example the $^4I_{9/2}$ ground state is split into five Stark levels.

3.1. Absorption spectra and oscillator strengths

In figure 1 we show the unpolarized optical absorption spectra of NGO (σ, π-configuration) and LGO:Nd measured at 10 and 300 K over the 200–900 nm range. Two other very weak absorption bands, not shown in that figure, at about 1625 and 2420 nm have also been detected for NGO.

The NGO single-crystal absorption edge is at about 220 nm (45 500 cm^{-1}). Due to the high Nd^{3+} concentration most of the possible zero-phonon f–f electronic transitions in that region can be clearly seen. Since some of these bands are very narrow they have to be measured with a high spectral resolution. At low temperatures, the structure of the optical absorption spectrum reflects that of the excited states. Here we note that the absorptions from the fundamental level to $^2F_{5/2}$, $^2P_{3/2}$, $^2P_{1/2}$, $^4F_{9/2}$, $^4F_{3/2}$, etc, excited states, consist of three, two, one, five, two, etc, bands respectively, as expected for a low-symmetry site. The absorption energy and labelling of the levels are given in table 1. In some cases the

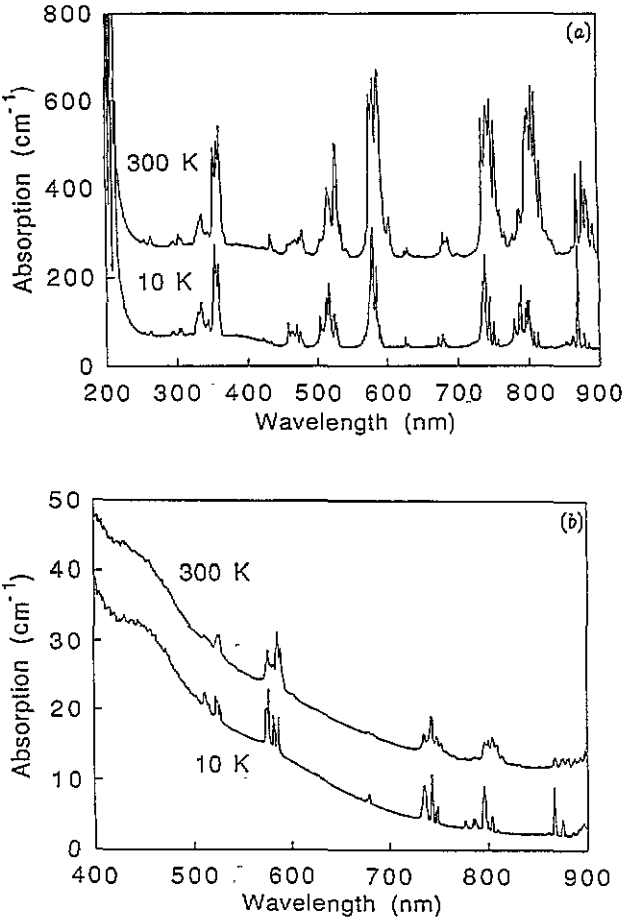

Figure 1. (*a*) The unpolarized (σ, π-configuration) optical absorption spectra of NGO measured at two different temperatures. (*b*) The unpolarized optical absorption spectra of neodymium-doped LGO measured at two different temperatures.

individual transitions cannot be resolved because of the band overlapping. In such cases the centroid of the band is given.

Some of the absorption bands are partially polarized. In figure 2(*a*) we present the $^4I_{9/2} \rightarrow {}^2D_{5/2}$ and $^2P_{1/2}$ absorption bands measured at 10 K with light polarized with the electric field either parallel, π, or perpendicular, σ, to the *c*-axis. The degree of polarization, P, at 10 K of the bands in the 350–900 nm region defined as $(I_\pi - I_\sigma)/(I_\pi + I_\sigma)$ is also given in table 1.

For LGO:Nd the poor optical quality of the samples produces strong light scattering in the high-energy spectral region such that we were only able to measure in the 430–900 nm region. The absorption energy and labelling of the levels are given in table 2. Although the lines are broader than for NGO, for example 0.6 nm versus 0.2 nm halfwidth for the $^4I_{9/2} \rightarrow {}^2P_{1/2}$ absorption band at 9 K, the close similarity in band positions and absorption strengths for both compounds confirms that, as expected, Nd impurity ions enter the LGO lattice at the La sites. For this compound we could not obtain a single crystal large enough to perform polarization experiments.

The thermal evolution of the absorption spectra of both samples was measured over the

Table 1. $NdGaO_3$. Energy levels (ν in cm^{-1}), polarization degree P at 10 K, σ, π-polarization experimental f oscillator strengths (in 10^{-8} units) and R (ratio of vibronic to zero-phonon band strengths).

Level	ν	P(10 K)	f(300 K)	f(300 K)/f(10 K)	R
$^2F_{3/2}$	39525	—	18.5	2.1	—
$^2F_{5/2}$	37735	—	52.2	2.65	—
$^2H_{11/2}$	34130	—	27	1.3	—
$^2D_{5/2,3/2}$	32785	—	60	1.4	—
$^2H_{9/2}$	31645	—	5.3	0.5	—
$^2L_{17/2,15/2}$					
$^4D_{7/2}$, $^2I_{13/2}$	30490	—	350	1	—
$^4D_{3/2,5/2}$, $^2I_{11/2}$	27933	—	1100	3.8	—
$(^2D, ^2P)_{3/2}$	26042	0	3.7	1	—
$^2D_{5/2}$	23753	0.65	3.1	0.4	—
	23641	−0.1			
$^2P_{1/2}$	23164	0.3	43	10.8	0.3
$^2K_{15/2}$, $^2G_{9/2}$ $(^2D, ^2P)_{3/2}$, $^4G_{11/2}$	21276	0.35	191	1.3	—
$^2K_{13/2}$, $^4G_{7/2,9/2}$	19194	0.3	657	2.05	—
$^4G_{5/2}$, $^2G_{7/2}$	17330	−0.1	1100	3.3	—
$^2H_{11/2}$	15748	0	14.7	2	0.1
	14916	0.25			
	14771	−0.1			
$^4F_{9/2}$	14725	0	63.5	3.7	—
	14684	0			
	14569	0			
$^4F_{7/2}$, $^4S_{3/2}$	13495	0.2	638	3.9	—
$^4F_{5/2}$, $^2H_{9/2}$	12422	0	612	4.4	—
$^4F_{3/2}$	*11521*	*0*	*208*	*3.6*	*0.75*
	11399	0			

9–300 K temperature range. On increasing the temperature we expect a progressive thermal population of the ground-state Stark levels governed by Boltzmann statistics, resulting in a decrease of the low-temperature spectrum and an increase in the lower-energy sides of some absorption bands. In our case a pattern of five absorption bands, corresponding to $^4I_{9/2}$ degeneracy, should develop with temperature for all the absorption bands.

The effect has indeed been observed and at temperatures close to 300 K any one $J \rightarrow J'$ absorption band consists of sets of five components corresponding to transitions from the five ground-state levels.

The thermal behaviour of the band at ≈432 nm is of special interest. It is due to transitions from the ground $^4I_{9/2}$ multiplet to the only experimentally accessible singlet $^2P_{1/2}$ state. Thus, at 10 K the spectrum consists of one subband (see figure 2(*a*)), the number of subbands increasing to five at 300 K due to the thermal population of the ground-state sublevels. In figure 2(*b*) we show the polarized spectrum of the $^4I_{9/2} \rightarrow {}^2P_{1/2}$ transitions at 300 K to illustrate this point. Combining the two polarizations we obtain five bands (labelled L1–5 in figure 2(*b*)) separated by $\Delta_i = 90$, 180, 430 and 545 ± 5 cm^{-1} corresponding to the Stark splitting of the $^4I_{9/2}$ ground state for NGO in agreement with the inelastic neutron scattering results in [4].

From the thermal evolution of the Nd^{3+} absorption bands for LGO we obtain $\Delta_i =$ 85, 155, 450 and 535 ± 5 cm^{-1} which are very similar to those for NGO.

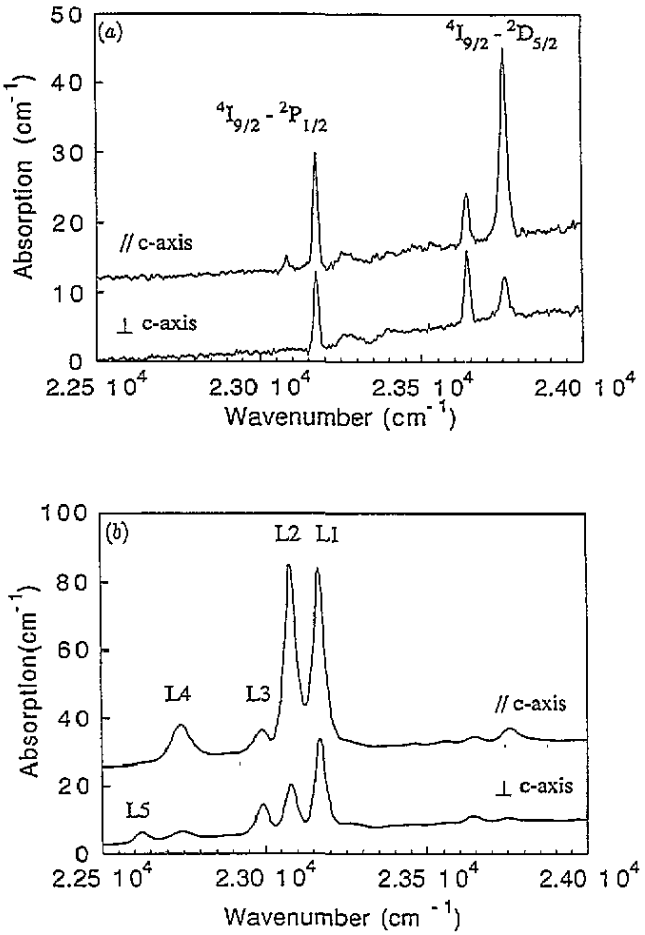

Figure 2. The polarized spectra corresponding to the $^4I_{9/2} \rightarrow ^2P_{1/2}$, $^2D_{5/2}$ transitions for NGO (*a*) measured at 10 K, (*b*) measured at 300 K.

The temperature evolution of the absorption bands is also interesting. Although the bands widen with temperature, their peak positions, determined, for example, in the case of the $^4I_{9/2} \rightarrow {}^2P_{1/2}$ transition for NGO with an accuracy better than 0.1 nm, do not change with temperature. This is normally expected for zero-phonon lines but for NGO the temperature dependence of the absorption band intensities is abnormal.

In figure 3 we plot the temperature dependence of the integrated absorption (σ, π-configuration) for each of the five components of the $^4I_{9/2} \rightarrow {}^2P_{1/2}$ transition. It can be clearly seen that, for example, the relative intensity of the subband L1 does not obey the expected Boltzmann distribution function for the density of states in the ground state. Consequently its oscillator strength has to be temperature dependent. We also observe an increase of more than ten times for the total area under the $^4I_{9/2} \rightarrow {}^2P_{1/2}$ absorption band from 10 to 300 K while that of the $^4I_{9/2} \rightarrow {}^2D_{5/2}$ absorption band decreases.

We can analyse quantitatively this behaviour by calculating the transition 'oscillator strengths' from the area under the absorption bands through the following expression:

$$f = \frac{mc^2}{\pi e^2 N} \int \frac{2.303\mathrm{OD}(\lambda)}{L\lambda^2}\, \mathrm{d}\lambda \qquad (1)$$

Table 2. $LaGaO_3$:Nd. Energy levels (ν in cm^{-1}), experimental f_{exp} and calculated f_{the} oscillator strengths (in 10^{-8} units).

Level	ν	f_{exp}(300 K)	f(300 K)/f(10 K)	f_{the}
$^2P_{1/2}$	23226	72	1.3	53
$^2K_{15/2}$, $^2G_{9/2}$ (^2D, $^2P)_{3/2}$, $^4G_{11/2}$	—	—	—	—
$^2K_{13/2}$, $^4G_{7/2,9/2}$	19263	510	0.875	459
$^4G_{5/2}$, $^2G_{7/2}$	17166	1476	1.5	1480
$^2H_{11/2}$	15768	—	—	—
	14948			
	14921			
$^4F_{9/2}$	14793	40.5	1	41.4
	14723			
	14579			
$^4F_{7/2}$, $^4S_{3/2}$	13470	540	1.3	522
$^4F_{5/2}$, $^2H_{9/2}$	12400	490	1.6	530
$^4F_{3/2}$	11542	150	1	186
	11436			
	6615, 6548			
$^4I_{15/2}$	6486, 6310	—	—	—
	6202, 5999			
	5934, 5778			
	4344, 4231			
$^4I_{13/2}$	4193, 4146	—	—	—
	4034, 4018			
	3940			

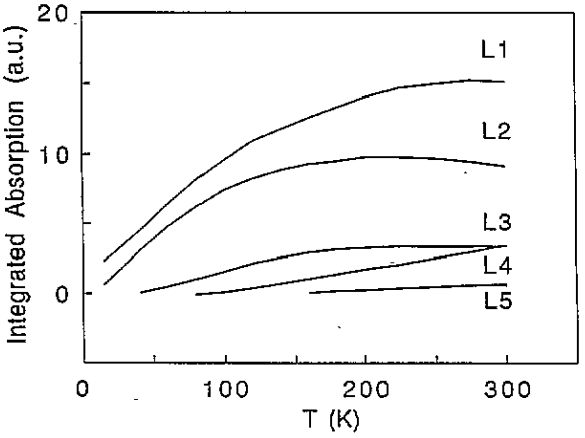

Figure 3. The temperature dependence of the integrated absorption (σ, π-configuration) of the Stark components of the $^4I_{9/2} \rightarrow {}^2P_{1/2}$ transition for NGO.

where m and e are the electron mass and charge respectively, c is the light velocity, OD(λ) the optical density as a function of wavelength λ and L the thickness of the sample. N is the number of absorbing ions in the unit volume.

In applying equation (1) we have to remember that the number of occupied states in

any of the five levels of the ground-state multiplet N_i depends on temperature according to Boltzmann statistics:

$$N_i(T) = N\mathrm{e}^{-(\Delta_i/kT)} / \sum_{i=1}^{5} \mathrm{e}^{-(\Delta_i/kT)} \tag{2}$$

where Δ_i are the energy differences between the ground and the ith level and k is the Boltzmann constant.

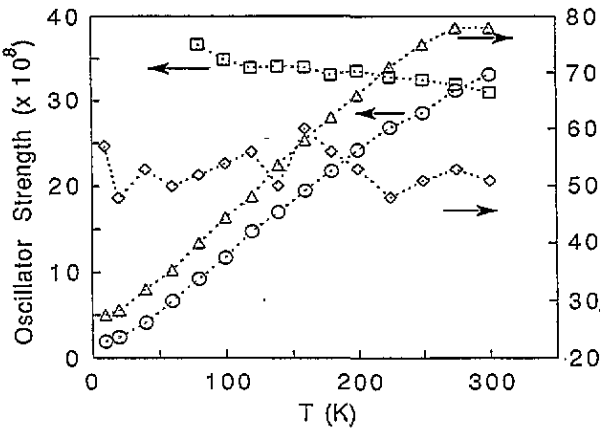

Figure 4. The temperature dependence of the oscillator strengths of some zero-phonon lines. ○, L1 and □, L2 lines of the $^4I_{9/2} \rightarrow {}^2P_{1/2}$ and △, the L1 line of the $^4I_{9/2} \rightarrow {}^4F_{3/2}$ transitions in NGO (σ, π-configuration). ◇, L1 line of the $^4I_{9/2} \rightarrow {}^2P_{1/2}$ transition for LGO.

In figure 4 we give the oscillator strengths as a function of temperature of some well resolved bands, calculated from the unpolarized absorption spectra using equations (1) and (2). There is a monotonic increase with temperature for the oscillator strength of the $^4I_{9/2} \rightarrow {}^2P_{1/2}$ L1 line for NGO, throughout the 9–300 K region. However that of line L2 is almost temperature independent, whereas that of line L3 decreases with temperature (not shown in the figure). The oscillator strength of the highest-energy, zero-phonon line of the $^4I_{9/2} \rightarrow {}^4F_{3/2}$ doublet also increases with temperature. In contrast, all the zero-phonon line oscillator strengths measured for LGO are temperature independent (see the evolution of the $^4I_{9/2} \rightarrow {}^2P_{1/2}$ L1 line for LGO in figure 4).

Due to band-overlap effects, it is sometimes difficult to resolve experimentally the contributions of individual zero-phonon lines for transitions to an excited level with high multipliticies. In such cases we can calculate a 'weighted averaged oscillator strength' by applying equation (1) to the entire absorption band.

Tables 1 and 2 give such 'oscillator strengths' for NGO and LGO, respectively, at 300 K together with their temperature dependences as given by the ratio between their values at 300 and 10 K. For LGO the f values of weak bands cannot be calculated accurately.

Comparing the f values of tables 1 and 2 we clearly observe a different behaviour for the NGO and LGO. Although the transition probabilities at 300 K are very similar for both compounds, for NGO most of the absorption bands decrease with temperature whereas they remain nearly temperature independent for LGO.

It is worth mentioning here that since the transition probabilities from each individual Stark level of the ground state to a given excited level need not necessarily be the same, the

integrated transition probability for a composite band can change with temperature even if their individual bands do not. This effect could explain, for example, the slight temperature dependence of some of the LGO f values listed in table 2.

3.2. LGO RT intensity parameters

For lanthanide trivalent ions the f–f spectra are mainly a result of forced electric dipole transitions due to mixing the $4f^N$ configuration with other configurations having opposite parity. Such mixing may be produced by either the odd-parity terms of the crystal-field potential (static contribution) or by non-totally symmetric lattice or cluster vibrations (dynamical contribution), the latter being generally more important for sites with inversion symmetry.

Judd and Ofelt [16, 17] developed a theory (J–O theory) to calculate f–f transition probabilities as a function of three parameters that account for both static and dynamic configuration mixing. It is interesting to remember here the assumptions made in the derivation of the J–O theory. First the odd-parity configurations which mix with the 4f configuration are assumed to be degenerate and spread over a wide energy range. Secondly, the 4f-mixing configuration energy differences are assumed equal for all the 4f levels. Thirdly, all the M_J levels are assumed equally populated.

For Nd^{3+} ions the first excited $4f^25d$ and $4f^25g$ configurations are expected to be over 50 000 cm^{-1} higher than the ground state, so for the lowest 4f levels it can be safely assumed that the first two assumptions hold.

Although the third assumption is not entirely satisfied even at 300 K it is customary to analyse Nd^{3+} RT absorption spectra using J–O theory. For LGO we have experimental evidence for oscillator strengths of the $J \rightarrow J'$ absorption bands being slightly dependent on temperature. Thus we can assume that the 300 K spectra reproduce well the situation at high temperatures needed for J–O theory to be applied.

Within the frame of J–O theory the 'oscillator strength' $f(J, J')$ of the $J \rightarrow J'$ transition (at a mean frequency ν) is given by

$$f(J, J') = \frac{8\pi^2 m\nu}{3h(2J+1)e^2n^2}\left[X_{ed}S_{ed} + X_{md}S_{md}\right] \tag{3}$$

where n is the refraction index and we define $X_{ed} = n(n^2+2)^2/9$ and $X_{md} = n^3$. The magnetic dipole transitions only give here a negligible contribution to the absorption bands.

The electric dipole line strength S_{ed} is given by

$$S_{ed}(J, J') = e^2 \sum_{t=2,4,6} \Omega_t \left|\langle (SL)J||U^{(t)}||(S'L')J'\rangle\right|^2 \tag{4}$$

where Ω_2, Ω_4, Ω_6 are three parameters (J–O parameters) to be obtained from a comparison with experimental results. The reduced matrix elements of the unit tensor $U^{(t)}$ ($t = 2, 4, 6$) are almost insensitive to the ion environment. The values given in [18] have been used in the calculations.

The J–O parameters, found by a least-squares fit of the calculated 'f' values given by equation (3) to the experimental ones, are compared in table 3 with those for other oxide matrices. The oscillator strengths calculated using these values are also given in table 2. The root mean square value of the fitting is $\approx 4 \times 10^{-7}$ which is within the usual range for this kind of analysis.

Table 3. Judd–Ofelt parameters of Nd^{3+} (10^{20} cm^2). For $NdGaO_3$ the polarization is indicated (see the text).

	Ω_2	Ω_4	Ω_6	References
$LaGaO_3$	2.1	2.4	2.3	This work
$NdGaO_3$	−0.05 (π)	1.3 (π)	0.9 (π)	This work
	0.25 (σ)	1.15 (σ)	0.85 (σ)	This work
	0.46 (eff)	3.6 (eff)	2.6 (eff)	This work
YSZ	1.1	1.24	1.23	[19]
LaF_3	0.35	2.6	2.5	[20]
$YAlO_3$	1.25	4.7	5.85	[21]

3.3. Vibronic side bands

For NGO all the absorption bands, besides the electronic zero-phonon transitions, have phonon side bands at shortwave. In contrast, only very weak ones at noise level are seen for LGO. These side bands can be observed in the spectra shown in figure 2 but the most pronounced ones correspond to the $^4I_{9/2} \rightarrow {}^4F_{3/2}$ transition. In figure 5 we present this absorption band measured at 10 K. It has a clearly resolved structure up to energies of $\approx$450 cm^{-1} greater than the zero-phonon line.

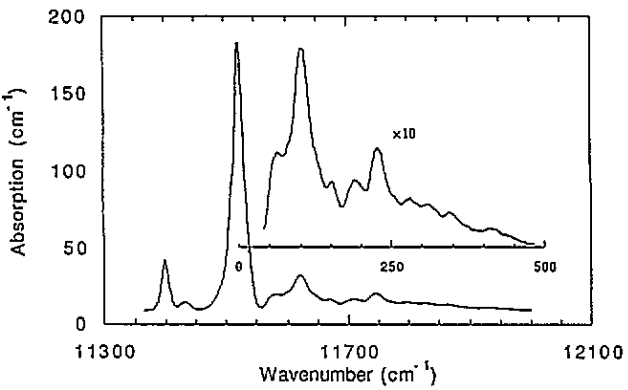

Figure 5. The zero-phonon and vibronic bands corresponding to the $^4I_{9/2} \rightarrow {}^4F_{3/2}$ transition for NGO measured at 10 K.

In table 1 we give the ratio of the integrated vibronic band intensity I_{vib} to the zero-phonon line intensity I_{zp}, $R = I_{vib}/I_{zp}$ at 10 K for those absorption bands whose vibronic spectrum and zero-phonon bands are better resolved. At higher temperatures the bands broaden and the vibronic lines corresponding to the other zero-phonon transitions from thermally populated ground-state Stark levels overlap each other making it difficult to determine the individual contributions.

Usually, two different contributions to the vibronic transition probability have been distinguished, the M and the Δ processes [13]. The former is due to forced dipolar transitions induced by coupling with vibrational modes. The oscillator strength of the vibronic transition is proportional, independent of the rare-earth site symmetry, to the $U^{(2)}$ reduced element in equation (4) and hence it is expected to be larger for hypersensitive transitions [22]. We have seen well resolved absorption vibronic side bands precisely in

transitions with $||U^{(2)}|| = 0$ so we can conclude that the M process is very inefficient for NGO.

The Δ process originates from the displacement of the excited-state configurational coordinate equilibrium position relative to that of the ground state. Within the configurational-coordinate model we can obtain an 'effective Huang–Rhys factor S_0' giving us a measure of the electron–phonon coupling.

At $T = 0$ it can be obtained from the expression

$$I_{tot}/I_{zp} = 1 + I_{vib}/I_{zp} = \exp(S_0). \tag{5}$$

From data given in table 1 we obtain S_0 values between 0.1 and 0.6.

The vibronic structure consists of a one-phonon density-of-states-like spectrum with some well resolved peaks. The peak positions coincide approximately with the phonon frequencies obtained by Raman and infrared techniques [23] (see table 4). It is interesting to note that the vibronic sidebands appear in the energy region of the phonon modes involving stretching or bending of the Nd–O bond. The stretching of the Ga–O octahedra which appears in the 360–620 cm^{-1} region [6] has a negligible contribution to the vibronic bands. The Raman spectra of both compounds, including symmetry assignments, will be reported in a forthcoming publication [24]. As expected the phonon frequencies of the LGO compound are very similar to those of NGO owing to the small isotopic shift.

Table 4. NGO phonon frequencies in cm^{-1}.

i.r. [23]	Raman [23]	Vibronic (this work)
607	—	—
548	—	—
510	—	—
455	469	—
—	452	—
435	—	—
—	410	406
390	—	—
—	361	—
357	—	—
—	346	—
—	340	340
325	—	—
308	—	308
285	289	277
220	—	222
—	214	—
—	200	—
185	180	184
—	169	—
—	145	148
—	135	—
—	92	98
—	—	56

3.4. Emission spectra and lifetimes

No emission has been detected for NGO even at lower temperatures. In contrast, emissions from the $^4F_{3/2}$ level were detected at temperatures between 9 and 300 K for LGO. At low temperatures the emission spectra reflect the Stark structure of the final level. As shown in figure 6 the structure of the $^4F_{3/2} \rightarrow {}^4I_{9/2}$ emission band corresponds to the crystal-field levels of the ground state, whereas those of the $^4I_{11/2}$ level are 50, 100, 150, 230 and 315 ± 5 cm^{-1}, respectively. The decay curve of the emission is exponential with a decay time independent of temperature of 230 μs.

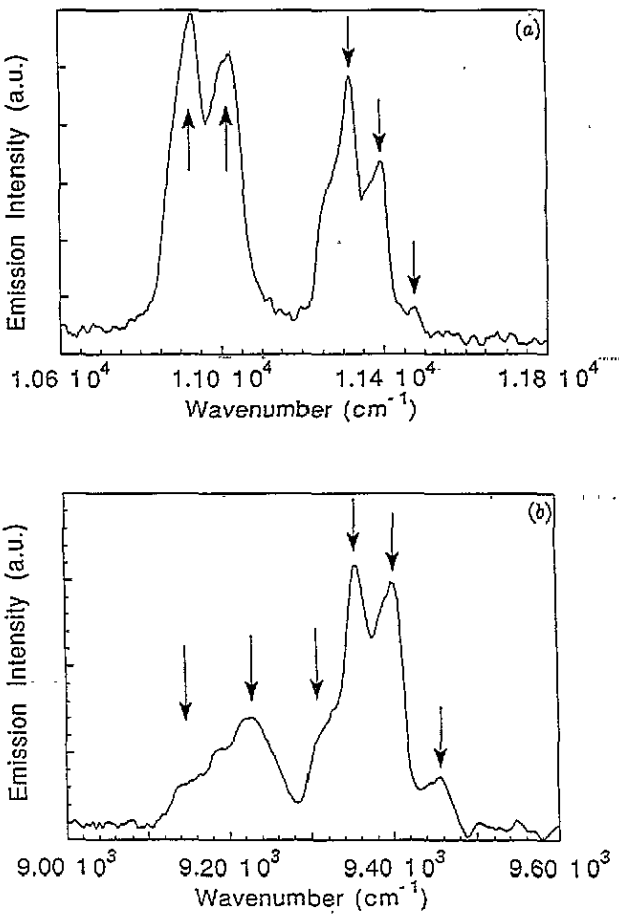

Figure 6. Neodymium-doped LGO emission bands measured at 10 K: (*a*) $^4F_{3/2} \rightarrow {}^4I_{9/2}$ transition; (*b*) $^4F_{3/2} \rightarrow {}^4I_{1/2}$ transition. Stark components are given by arrows.

The Ω_t values obtained from the absorption data can now be used to calculate the spontaneous emission probabilities $A(J, J')$ of the different electronic transitions, which are given by the expression

$$A(J, J') = \frac{64\pi^4\nu^3}{3(2J+1)hc^3}\left[X_{ed}S_{ed} + X_{md}S_{md}\right] \tag{6}$$

and are related to the radiative lifetime τ_R of the excited state 'J' by

$$\frac{1}{\tau_R} = \sum_{J'} A(J, J') \tag{7}$$

where the summation is over the electric and magnetic dipole transitions to all terminal states 'J''. This gives a calculated radiative lifetime of $\approx$255 μs which coincides with the experimental one. It is interesting to notice that the $^4F_{3/2}$ level emission probability does not depend on Ω_2.

The difference between calculated and experimental emission decay times is negligible, so the emission quantum efficiency of the $^4F_{3/2}$ level is close to one. In accordance the relaxation time is temperature independent and non-radiative decay via multiphonon relaxation is negligible. This is expected because the energy gap between the emitting $^4F_{3/2}$ level and the next one below it, $^4I_{15/2}$, is $\approx$5000 cm^{-1}, ten times larger than the most energetic interacting phonon.

3.5. NGO RT polarized absorption

We could not perform polarization studies for LGO. Thus, the analysis of the Nd^{3+} intensity parameters has been done within the frame of J–O theory for isotropic systems.

For NGO, the polarization dependence of the Nd^{3+} absorption bands has been measured in the 350–900 nm range at different temperatures. Due to the thermal population of the $^4I_{9/2}$ Stark levels, the polarization degree of the bands given in table 1 for 10 K changes with temperature. In table 5 we present the 300 K experimental oscillator strengths obtained from equation (1) for both σ- and π-polarizations.

Table 5. $NdGaO_3$. Polarization dependence of the Nd^{3+} absorption bands at 300 K. Experimental (f_{exp}) and calculated (f_{the}) oscillator strengths (in 10^{-8} units).

	f_{exp}	f_{the}	f_{exp}	f_{the}
Level	π-polarization		σ-polarization	
$(^2D, ^2P)_{3/2}$	3.9	4.9	3.5	4.2
$^2D_{5/2}$	3.3	3.7	2.9	3.4
$^2P_{1/2}$	61	89	26	74.5
$^2K_{15/2}$, $^2G_{9/2}$	221	140	167	122
$(^2D, ^2P)_{3/2}$, $^4G_{11/2}$				
$^2K_{13/2}$, $^4G_{7/2,9/2}$	691	589	624	536
$^4G_{5/2}$, $^2G_{7/2}$	1000	1008	1200	1207
$^2H_{11/2}$	18.5	15	11	13.5
$^4F_{9/2}$	64	53	60	49
$^4F_{7/2}$, $^4S_{3/2}$	665	645	615	595
$^4F_{5/2}$, $^2H_{9/2}$	645	715	580	640
$^4F_{3/2}$	220	300	200	255

Next, we perform the analysis of the oscillator strengths using the J–O theory adapted for uniaxial systems [25]. For the uniaxial crystal and only retaining the relevant electric-dipolar contribution equations (3) and (4) transform into

$$f_{q,ed}(J, J') = X_{q,ed}\frac{8\pi^2 m\nu}{h(2J+1)}\sum_{t=2,4,6}\Omega_{q,t}\left|\langle (SL)J||U^{(t)}||(S'L')J'\rangle\right|^2 \tag{8}$$

with

$$q = \begin{cases} 0 & \pi\text{-polarization} \\ \pm 1 & \sigma\text{-polarization} \end{cases}$$

and

$$X_{q,ed} = \frac{(n_q^2 + 2)^2}{9n_q} \qquad n_0 = n_e \text{ and } n_{\pm 1} = n_0.$$

For the refraction index we have used the value obtained with unpolarized white light, $n_0 = n_e = 2.13$, and for the reduced matrix elements of the unit tensors $U^{(t)}$ ($t = 2, 4, 6$) those of [18].

The J–O parameters, found by a least-squares fit of the calculated f values given by equation (8) to the experimental ones, are given in table 3. It can be seen that the anisotropy is much larger for Ω_2 than for Ω_4 and Ω_6 which are nearly isotropic. Ω_2 is negative and close to zero for π-polarization. We think that the Ω_2 polarization dependence is related to the hypersensitivity effect of some optical transitions to be discussed later on.

The oscillator strengths calculated using these J–O intensity parameters are also given in table 5. The root mean square values of the fitting are ≈ 6 and 5×10^{-7} for π- and σ-polarization respectively, within the usual range for that kind of analysis.

To compare with the 'unpolarized' J–O parameters for LGO we have calculated the effective isotropic intensity parameters defined as

$$\Omega_t^{eff} = \Omega_{\pi,t} + 2\Omega_{\sigma,t} \tag{9}$$

given in table 3.

4. Discussion and conclusions

In the preceding section we have reported on the spectroscopic properties of Nd^{3+} in two compounds having a similar crystal structure with only the ion concentration being different. The level positions and crystal-field splittings are very similar for both compounds. Small shifts toward lower energies for the electronic transitions between individual crystalline Stark components for NGO ($\approx$20 to 60 cm^{-1}) can be attributed to an increase in the covalency degree (nephelauxetic effect) due to the smaller lattice parameters of NGO.

In addition the absorption bands are noticeably narrower for NGO than for LGO ($\approx$10 cm^{-1} for the $^4I_{9/2} \rightarrow {}^2P_{1/2}$ band at 9 K for NGO versus $\approx$30 cm^{-1} for LGO). We think that the poor quality of the LGO crystal could in principle explain these differences in halfwidth.

In agreement with the low magnitude of the ion–ion magnetic interactions we have not observed any band splitting for NGO that could be associated with ion–ion interactions. The effect of concentration on the electron eigenvalues is negligible. However, it has a relatively large influence on the eigenstates: one experimental finding that supports this assertion is the strong emission quenching for NGO. Emisson concentration quenching for Nd^{3+} compounds is a well known effect and it may proceed via a pair-relaxation mechanism if there is an intermediate level at exactly half of the gap between the ground state and the emitting level [26]. This is the case for the $^4I_{15/2}$ level. The process is resonant and requires no phonon interaction. Since it is very sensitive to the ion–ion distance, to gain more insight

on the effect of concentration quenching in gallates it would be very interesting to study the lifetime evolution as a function of the Nd concentration for values higher than 1% for LGO.

In any case when we compare the RT intensity parameters of LGO and NGO (see table 3) we observe a difference in Ω_2 that could be related to the well known effect of hypersensitivity of some f → f transitions. In fact the transitions obeying the selection rules $2 \geqslant |\Delta J|$ and $\Delta S = 0$ have an extraordinarily large dependence on their environment. These are the selection rules for just the $||U^{(2)}||$ reduced element multiplying Ω_2 in equation (4). Different theoretical approaches to account for the hypersensitivity effect have been reviewed in [27].

Changes in the Ω_2 values are expected when either the ion–ligand distance or the ion site symmetry changes. The point group of Nd^{3+} ions is C_s both for NGO and LGO and the crystal field is also similar for both compounds as indicated by the similarity of the Stark splittings. Consequently it is not easy to explain the changes in Ω_2 in the light of current theories for hypersensitive behaviour.

Moreover, we have seen that the intensities of almost all the absorption bands for NGO are lower at low temperature than the corresponding ones for LGO, and increase as the temperature rises until they approach the LGO values. For the latter they remain nearly constant over the entire temperature range. Of special interest is the different behaviour of the oscillator strengths of some well resolved zero-phonon lines as the temperature evolves. As far as we know this is a very unusual finding that questions the possible influence of ion concentration on the transition probability.

Concentration enhancement of vibronic lines in the excitation spectra has been observed for several ions (Eu^{3+} [28], Gd^{3+} [29] and Pr^{3+} [30]) and tentatively assigned to a superexchange interaction between rare-earth ions. However in a recent paper Blasse and co-workers [31] have shown that the supposed concentration enhancement is the result of a misinterpretation of the experimental data due to saturation effects. We have studied the absorption spectra which avoids that problem.

In our case exchange interaction between Nd^{3+} ions seems also to be the best explanation for the different behaviour of LGO and NGO. For NGO the Nd^{3+} interionic distances are short enough to allow for some overlap between their electronic states. The size of the 4f wavefunction drops to 1% at 2.5 Å [32] while that of the 5d configuration extends up to about 8 Å [33]. Although f–f overlap is very small as indicated by the low value of the magnetic exchange integral d–d exchange can be large.

The effect of excited configuration exchange on the f–f transition probabilities was studied several years ago by Danielmeyer [34]. He suggested that exchange between ion pairs may take place through the more extended 5d states. The exchange-coupled 5d states are mixed by odd static crystal-field terms or phonons with the f states producing the forced electric dipolar transitions predicted by the J–O theory. The 5d wavefunction of one ion is mixed with the 4f of the next one thus increasing the transition probabilities in stoichiometric materials in analogy with the one-centre parity crystal-field mixing effect. Danielmeyer's hypothesis was contested by Auzel's experimental study for some Nd^{3+} compounds where oscillator strengths were found to be essentially concentration independent [35].

For NGO we have observed a decrease in the oscillator strengths rather than the increase predicted by 5d exchange theory. In any case there is the anomalous temperature dependence of the transition probabilities. Although at present we have not been able to work out a theoretical explanation for this unusual behaviour all the experimental facts point towards a predominant role of an electron–phonon coupling with the f–f transition probabilities for NGO. Such a predominance might be anticipated if we realize that configurational mixing

produces the main contribution to the oscillator strength of rare earths and that the excited configurations of nearest-neighbour Nd^{3+} ions are probably coupled by relatively strong superexchange interactions through common oxygen ions.

If follows, therefore, that the 5d excited state for NGO is an exciton-like state. Since for the perovskite structure the rare-earth sublattice is nearly cubic the exciton NGO states have a much higher symmetry than the LGO localized states. Accordingly, with this model we should expect a reduction rather than an enhancement of the oscillator strengths of some transitions on going from the diluted to the concentrated compound, as has been observed.

Superexchange interactions are highly anisotropic and consequently they are also strongly dependent on the oxygen ion positions. In the perovskite lattice large dynamic deformations of the oxygen sublattice take place. In fact the collective rotations of the oxygen octahedra produce the rich variety of structural phase transitions for this family of compounds. Thus phonon modulation of the superexchange coupling between the 5d Nd^{3+} excited states could explain on the one hand the observation of relatively large vibronic spectra for NGO and their absence in neodymium-doped LGO and on the other hand the large temperature dependence of some transition probabilities for NGO. The presence of only those phonon modes modulating the Nd–O bonding in the vibronic structure is also in agreement with this picture.

Acknowledgments

This work was supported by CICYT (Spain) grant MAT 92-0225. One of us, LET, would like to thank the European Community for the grant CIPA-CT92-2103.

References

[1] Bartolomé F, Kuz'min M D, Merino R I and Bartolomé J 1994 *IEEE Trans. Magn.* **MAG-30** 960
[2] Siegal M P, Phillips J M, Hebard A F, van Dover R B, Farrow R C, Tiefel T H and Marshall J H 1991 *J. Appl. Phys.* **70** 4982
[3] Phillips J M, Siegal M P, van Dover R B, Tiefel T H, Marshall J H, Brandle C D, Berkstresser G, Strauss A J, Fahey R E, Sengupta S, Cassanho A and Jensen H P 1992 *J. Mater. Res.* **7** 2650
[4] Podlesnyak A, Rosenkranz S, Fauth F, Marti W, Furrer A, Mirmelstein A and Scheel H J 1993 *J. Phys.: Condens. Matter* **5** 8973
[5] Marti W, Fischer P, Altorfer F, Scheel H J and Tadin M 1994 *J. Phys.: Condens. Matter* **6** 127
[6] Calvani P, Capizzi M, Donato F, Dore P, Lupi S, Maselli P and Varsamis C P 1991 *Physica C* **181** 289
[7] Zhang Z M, Choi B I, Flik M I and Anderson A C 1994 *J. Opt. Soc. Am.* B **11** 2252
[8] Sasaura M, Miyazawa S and Mukaida M 1990 *J. Appl. Phys.* **68** 3643
[9] Dube D C, Scheel H J, Reaney I, Daglish M and Setter N 1994 *J. Appl. Phys.* **75** 4126
[10] McClure D S 1975 *Optical Properties of Ions in Solids* ed B di Bartolo (New York: Plenum) p 259
[11] Yen W M and Selzer P M (ed) 1986 *Laser Spectroscopy of Solids (Topics in Applied Physics 49)* (Berlin: Springer)
[12] Henderson B and Imbush G F (ed) 1989 *Optical Spectroscopy of Inorganic Solids (Oxford Science Publications)* (Oxford: Clarendon) ch 10
[13] Blasse G 1992 *Int. Rev. Phys. Chem.* **11** 71
[14] Lempicki A and McCollum B C 1979 *J. Lumin.* **20** 311
[15] Geller S 1957 *Acta Crystallogr.* **10** 243
[16] Judd B R 1962 *Phys. Rev.* **127** 750
[17] Ofelt G S 1962 *J. Chem. Phys.* **37** 511
[18] Carnall W T, Croswhite H and Croswhite H M 1978 *Argonne National Laboratory Report* ANL-78-XX-95
[19] Merino R I 1993 *Thesis* University of Zaragoza
[20] Krupke W F 1966 *Phys. Rev.* **145** 325

[21] Weber M J, Varitimos T E and Mistanger B H 1973 *Phys. Rev.* B **8** 47
[22] Judd B R 1980 *Phys. Scr.* **21** 543
[23] Saine M C, Husson E and Brusset H 1981 *Spectrochim. Acta* A **38** 19
[24] Laguna M A, Sanjuán M L, Orera V M, Bartolomé J and Bartolomé F 1995 to be published
[25] Dai H and Stafsudd O M 1991 *J. Phys. Chem. Solids* **52** 367
[26] Lempicki A 1977 *Opt. Commun.* **23** 376
[27] Peacock R D 1975 *Struct. Bonding* **22** 83
[28] de Mello Donegá C, Meijerink A and Blasse G 1992 *J. Phys.: Condens. Matter* 4 8889
[29] Blasse G, Bixner L H and Hyatt G 1989 *Chem. Phys. Lett.* **164** 617
[30] de Mello Donegá C, Lambaerts H, Meijerink A and Blasse G 1993 *J. Phys. Chem. Solids* 54 873
[31] de Mello Donegá C, Meijerink A and Blasse G 1994 *J. Lumin.* **62** 189
[32] Krupke W F 1966 *Phys. Rev.* **145** 325
[33] Weber M J, Varitimos T E and Mistanger B H 1973 *Phys. Rev.* B **8** 47
[34] Danielmeyer H G 1976 *J. Lumin.* **12/13** 179
[35] Auzel F 1976 *IEEE J. Quantum Electron.* **QE-12** 258